

Percolative Conduction in Semiconducting Liquid Selenium-Thallium Mixtures*

R. B. Pettit and William J. Camp

Sandia Laboratories, Albuquerque, New Mexico 87115

(Received 24 March 1975)

We report accurate measurements of the electrical conductivity of the semiconducting liquid $\text{Tl}_x\text{Se}_{1-x}$ over the temperature range $250^\circ\text{C} \lesssim T \lesssim 500^\circ\text{C}$, and composition range $0.002 \leq x \leq 0.377$ (as well as $x=0$). The conductivity is thermally activated for all temperatures and compositions studied and its behavior is consistent with a changeover in conduction mechanism as x increases from zero. We interpret the $x > 0$ results in terms of percolative hopping.

In this paper, we report the first measurements of the electrical conductivity of the semiconducting binary liquid $\text{Tl}_x\text{Se}_{1-x}$ in the small- x (low Tl concentration) region. The electrical properties of pure liquid Se have been studied by a number of workers,¹⁻³ as have those of $\text{Tl}_x\text{Se}_{1-x}$ near and above stoichiometry, $x = \frac{2}{3}$.⁴⁻⁶ However the behavior of the dilute binary ($x \geq 0$) exhibits several novel features, discussed below, which are neither present in nor expected from the properties of pure Se or those of the binary alloy near stoichiometry.⁷

We have measured the electrical conductivity in the temperature range $250^\circ\text{C} \leq T \leq 500^\circ\text{C}$, and concentration range $0.002 \leq x \leq 0.38$ as well as at $x=0$ (pure Se). Our experimental apparatus and methods have been described in detail elsewhere.⁷ In Fig. 1 we show our results for the conductivity of the binary as a function of inverse temperature for values of the concentration ranging from 62.28 at.% Se ($x=0.3772$) to 99.80 at.% Se ($x=0.002$) as well as for nominally pure Se ($x=0$).⁸ (We note that materials used in these measurements were at least of 99.9999% metallic purity in all cases.) The experimental points lie entirely on the curves drawn, and experimental uncertainties of 1.0% in the conductivity and 3.0 K in the absolute temperature are less than the width of the drawn lines. Note the existence of a large immiscibility region in Fig. 1. In Ref. 7, we described the accurate determination of this phase boundary for both conductivity-temperature and concentration-temperature diagrams.⁹

Throughout the temperature and concentration range studied, the conductivity was found (with high precision) to be thermally activated:

$$\sigma(x, T) = \Sigma(x) e^{-\Delta(x)/kT}. \quad (1)$$

For pure Se ($x=0$) we find $\Sigma(0) \approx 320 (\Omega \text{ cm})^{-1}$ and $\Delta(0) \approx 1.05 \pm 0.02 \text{ eV}$, in agreement with previous work.^{2,3} The concentration dependences of $\Delta(x)$

and $\ln \Sigma(x)$ are shown in Fig. 2. The activation energy Δ decreases abruptly from 1.05 eV at $x=0$ to 0.53 eV at $x=0.002$, the smallest nonzero concentration studied, and thereafter decreases only slightly with increasing x to a value $\Delta = 0.43 \text{ eV}$ at $x=0.377$. On the other hand $\ln \Sigma$ decreases from 5.77 at $x=0$ to -0.81 at $x=0.002$. Thereafter, $\ln \Sigma$ increases very rapidly with increasing x to 9.74 at $x=0.377$.

It is particularly enlightening to view the behavior of $\ln \Sigma$ as a function of $r_s [= (3/4\pi\rho)^{1/3}$, where ρ is the Tl-atom density] which is a measure (about half) of the average distance between Tl atoms. This is displayed in Fig. 3. Note that at large r_s , $\ln \Sigma$ is a linearly decreasing function

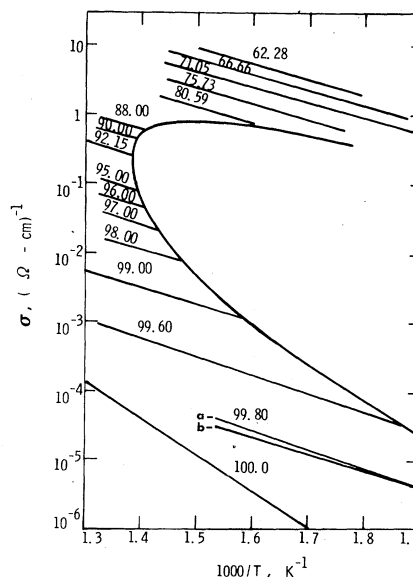


FIG. 1. The electrical conductivity of selenium-thallium mixtures at fixed composition (labeled in atomic percent selenium) as a function of the inverse temperature. At 99.80 at.% selenium, curve *a* is the total conductivity while curve *b* represents the thallium contribution to the conductivity. Note the large immiscibility region for temperatures below 722°K .

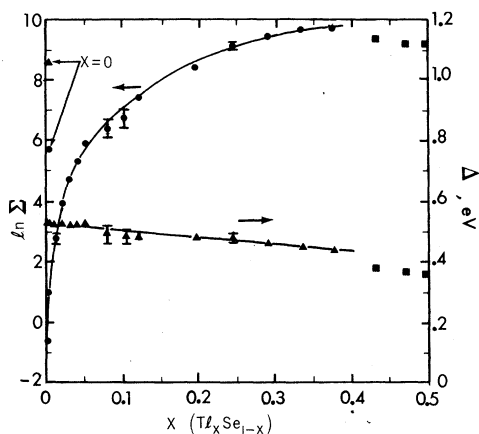


FIG. 2. The concentration dependence of the conductivity prefactor and activation energy as determined in this report (circles and triangles) and elsewhere (Ref. 6) (squares). The increased measurement error near the critical composition (~ 92 at. % Se) results from the limited temperature range of the data (only about 50°C).

of r_s . At smaller r_s , $\ln\Sigma$ increases more rapidly as r_s decreases. The linear range extends from the smallest nonzero concentrations to about 1.5–2.0 at. % Tl.

We have chosen to model the $\text{Tl}_x\text{Se}_{1-x}$ system for small x by assuming the presence of two mechanisms for transport: (i) "band" conduction due to the Se bands, which we assume for small x are unaffected by the presence of the Tl atoms; and (ii) "hopping" conduction by carriers associated with the Tl atoms. Our results are consistent with two distinct possibilities for the impurity-hopping mechanism. Namely, this mechanism could be phonon-assisted hopping conduction¹⁰ of carriers in a "band" of width much less than kT introduced at the Fermi level by the Tl atoms (which we assume to enter in the +1 state); or this mechanism could be resonant hopping by carriers in an impurity band located midway between the Fermi level and one of the mobility edges.¹ Although the spatial dependence of the hopping matrix elements is the same for both mechanisms, the measured activation energy in the resonant-hopping case is attributed to the energy required to promote a carrier into the impurity band, whereas in the phonon-assisted case, it is associated with the hopping barrier. Since both mechanisms are consistent with our results, we do not distinguish between them in our analysis, but rather refer to a hopping mechanism covering both possibilities. (Below we discuss planned experiments to distinguish which mech-

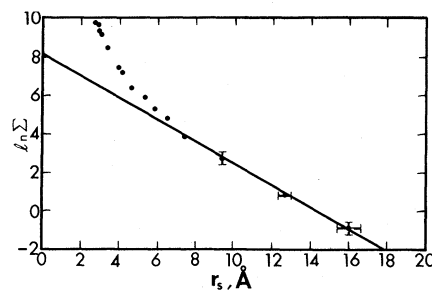


FIG. 3. The behavior of $\ln\Sigma$ as a function of half the average thallium atom spacing, r_s . The linear portion of the data has been extrapolated to $r_s = 0$.

anism is actually operative.)

Thus we have the standard formulas for the conductivity and thermopower,⁹

$$\sigma = \sigma_1 + \sigma_2, \quad Q = (\sigma_1 Q_1 + \sigma_2 Q_2) / (\sigma_1 + \sigma_2), \quad (2)$$

where the subscripts 1 and 2 respectively refer to the selenium and thallium mechanisms. Consider the conductivity. With our above assumptions, we have $\sigma_1 = 320e^{-1.05/kT}$ ($\Omega \text{ cm}$)⁻¹. At the smallest nonzero concentration studied ($x = 0.002$) the total conductivity is $\sigma = 0.51e^{-0.53/kT}$ ($\Omega \text{ cm}$)⁻¹. At the maximum temperature studied for this composition, the total conductivity is $\sigma(0.002) \cong 5.6\sigma_1$. Hence in interpreting our data at $x = 0.002$, we cannot ignore the selenium contribution to the total conductivity. The thallium contribution is shown in Fig. 1 (curve b, at 99.80 at. % Se) and values for $\ln\Sigma$ and Δ for the corrected curve are plotted in Figs. 2 and 3. (A much smaller correction factor was also applied at $x = 0.004$.) In interpreting our results for $x \geq 0.010$, we may ignore the Se contribution to the conductivity and analyze our data strictly in terms of the Tl contribution.

We thus assume that the conductivity of the dilute alloy is due to hopping of carriers. Assume that the rate for a carrier to hop from site i to site j , a distance R_{ij} away, is given by

$$\Gamma_{ij} = \Gamma_0 \exp[-R_{ij}/\xi - \Delta/(kT)], \quad (3)$$

where ξ is a characteristic decay length, and Δ is either the carrier hopping barrier energy (since we see no nonlinearity in the $\ln\sigma$ versus $1/T$ plots, we assume any disorder energy δ_{ij} is small compared to both Δ and kT , and thus ignorable) or the energy of promoting a carrier into the impurity band. We use the critical-path analysis (CPA) introduced by Ambegaokar, Halperin, and Langer (AHL)¹² to obtain the variation of hopping conductivity with impurity density. That the

CPA result is also an accurate estimate for σ at low impurity densities was explicitly demonstrated by Seager and Pike (SP),¹³ and by Ambegaokar, Cochran, and Kurkijärvi (ACK).¹⁴ According to AHL¹² the system may be replaced by a conductance network in which every pair of sites (i, j) is connected by a conductance $G_{ij} = e^2 \Gamma_{ij} / kT$. The essential step in CPA is to bound the conductivity by finding the path across the system with minimum impedance, and then to estimate the conductivity of the system as being proportional to the lowest conductance G_c in that path.

We proceed as follows. Place a sphere of radius r about every carrier site, then increase r to a critical value r_c chosen so that for $r < r_c$ there is no connected path across the system through overlapping spheres, and for $r \geq r_c$ there is at least one such path. Then, all the conductances along such a path equal or exceed

$$G_c = (e^2/kT) \Gamma_0 \exp(-2r_c/\xi - \Delta/kT), \quad (4)$$

and we estimate $\sigma \propto G_c$. The problem of finding r_c is treated in percolation theory, and has been numerically exactly solved by SP¹³ who find

$$2r_c = 1.4(3/4\pi\rho)^{1/3}, \quad (5)$$

where ρ is the number density of carriers (by assumption equal to the Tl atom density). Hence, according to our assumptions, the conductivity is estimated to be

$$\ln\sigma = \ln\sigma_0 - \Delta/kT - 1.4r_s/\xi, \quad (6)$$

where $r_s = (3/4\pi\rho)^{1/3}$ and σ_0 is a constant.¹³

By extrapolating the linear portion of the data in Fig. 3, we can obtain estimates for ξ and σ_0 . The $r_s = 0$ intercept of the extrapolated line yields $\ln\sigma_0 = 8.2 \pm 0.4$. From the slope we obtain $\xi = 2.5 \pm 0.2 \text{ \AA}$. The deviation from linearity observed in Fig. 3 may be expected on the basis of percolation theory. Basically, above a certain site density the CPA lower bound ceases to be an accurate estimate for σ . Simplistically, many parallel paths develop with conductances comparable to G_c , leading to an increase in σ .¹³ Returning to Fig. 3 we see that the breakaway from linearity occurs for $r_s \approx 8 \text{ \AA}$. On the basis of exact numerical techniques, SP¹³ showed that σ begins to deviate from the CPA estimate when r_s/ξ decreases through the range $3.0 < r_s/\xi < 5.0$. With $\xi = 2.5 \text{ \AA}$ our breakaway occurs near $r_s/\xi \approx 3.2$, in excellent agreement with SP.¹³ ACK¹⁴ have studied the hopping conductivity further into the nonlinear regime than have SP.¹³ Their estimates for the deviations from linearity are also

in reasonable agreement with ours. Considering that a power-law dependence on r_s/ξ may be expected in the prefactor σ_0 , and that such a dependence would tend to mask the actual breakaway from linearity, we see no reason to make more detailed comparisons with the results of SP¹³ and ACK.¹⁴

The behavior of σ for values of x in the range $0 < x < 0.002$, which we have not studied experimentally, is postulated by our model to be extremely interesting. Namely, for *extremely* small x the conductivity $\sigma = \sigma_1 + \sigma_2$ will be dominated by σ_1 (pure Se), and will show simple activated behavior with $\Delta \approx 1.05 \text{ eV}$ and $\Sigma \approx 320 (\Omega \text{ cm})^{-1}$. However for values of x such that $\sigma_1 \sim \sigma_2$, the conductivity will not be simply activated. Said differently, if we attempt to fit σ by the activated form $\Sigma e^{-\Delta/kT}$, both Σ and Δ will be strongly temperature dependent. In any case, assuming the validity of the two-mechanism model, we may estimate σ_2 even in the range $x \leq 0.001$ by subtracting the contribution σ_1 due to the selenium mechanism. Presumably, the percolative character of σ_2 will continue to be seen.

In summary, we have found evidence for impurity percolative conduction in $\text{Tl}_x\text{Se}_{1-x}$ for small x . To cement our conclusions requires (i) extensive thermopower measurements, and (ii) measurements of both conductivity and thermopower at lower Tl concentrations down to doping levels. Since the activation energy measured in a thermopower experiment is due solely to the cost of populating carrier levels, one would expect an "activated" thermopower $Q = Q_0 + A/T$ for the resonant-hopping case, while the thermopower would *not* be simply activated in the phonon-assisted hopping case. Such experiments are now in the preparation stage.

We have benefitted from conversations with D. Emin, G. E. Pike, C. H. Seager, J. P. Van Dyke, and especially M. L. Knotek.

*Research supported by the U. S. Energy Research and Development Administration.

¹The general reference for this work is N. F. Mott and E. A. Davis, *Electronic Processes in Non-Crystalline Semiconductors* (Clarendon, Oxford, England, 1971).

²H. W. Henkels and J. Maczuk, *J. Appl. Phys.* **24**, 1056 (1953).

³B. Lizell, *J. Chem. Phys.* **20**, 672 (1952).

⁴Y. Nakamura and M. Shimoji, *Trans. Faraday Soc.* **65**, 153 (1965).

⁵D. F. Stoneburner, AIME Trans. 233, 153 (1965).

⁶For a general review of extensive Russian work in this area, consult A. R. Regal *et al.*, in *Proceedings of the Tenth International Conference on the Physics of Semiconductors*, Cambridge, Massachusetts, 1970, edited by S. P. Keller, J. C. Hensel, and F. Stern, CONF-706801 (U.S. AEC Division of Technical Information, Springfield, Va., 1970).

⁷R. B. Pettit and W. J. Camp, Phys. Rev. Lett. 32, 369 (1974).

⁸Measurements of thermopower as a function of composition are in preparation. After completion of the studies of $x = 0.002$, our original cell broke; and further

studies await construction of new cells.

⁹In Ref. 7 we discuss the expected similarity between the critical properties of this transition and those of the liquid-vapor transition in metallic fluids.

¹⁰D. Emin, Phys. Rev. Lett. 32, 303 (1974), and private communication.

¹¹See Ref. 1.

¹²V. Ambegaokar, B. I. Halperin, and J. S. Langer, Phys. Rev. B 4, 2612 (1971).

¹³C. H. Seager and G. E. Pike, Phys. Rev. B 10, 1435 (1974).

¹⁴V. Ambegaokar, S. Cochran, and J. Kurkijärvi, Phys. Rev. B 8, 3682 (1973).

One-Dimensional Plasma as an Example of a Wigner Solid*

Bill Sutherland†

Institute for Theoretical Physics, State University of New York at Stony Brook, Stony Brook, New York 11794

(Received 24 April 1975)

In a previous Letter the author presented the exact ground-state wave function for a one-dimensional plasma with short-range polarization forces and a uniform background of opposite charge. In this Letter it is proven that the ground state has long-range crystalline order, and thus is an example of the Wigner solid. The n -particle density matrices are evaluated in closed form.

Some years ago, Wigner¹ realized that at sufficiently low densities a plasma of electrons immersed in a uniform neutralizing background of opposite charge would crystallize into a solid—the so-called Wigner solid. This crystalline state, or phase, may be expected to exist not only in the ground state, but also at finite temperatures.

If one considers instead the corresponding one-dimensional plasma of condenser plates with the Coulomb potential $V(x) = -|x|$, the situation is not so clear. There exist general theorems for short-range potentials which eliminate long-range order of the crystalline sort both at finite temperature and in the ground state. However, for an interaction as long range as the one-dimensional Coulomb potential, the general theorems give no guidance.

The thermodynamics of the classical one-dimensional plasma has been explicitly calculated,² and shown to have long-range order.³ It is the purpose of this Letter to demonstrate by an exact calculation that the ground state of the corresponding quantum plasma in one dimension also exhibits long-range crystalline order. This is one of the few examples of a continuous system which may be exactly solved and shown to have a broken continuous symmetry (translational invariance) in the ground state.

This work takes as its starting point the ground-state wave function of the one-dimensional plasma presented in the author's previous Letter.⁴ It was there shown that the function

$$\Psi = C \prod_{i < j} \theta_1(\pi(x_j - x_i)/L | i\gamma/L) \equiv C \prod_{i < j} \psi_{ij} \quad (1)$$

is the ground-state wave function and E_0 the ground-state energy for N fermions in one dimension with the Hamiltonian (periodic boundary conditions with period L)

$$H = -\sum_j \partial^2 / \partial x_j^2 + V, \quad (2)$$

where

$$V - E_0 = \sum_{i < j} [N\psi_{ij}'' / \psi_{ij} + 2\eta(N - 2)/L] = \Psi^{-1} \sum_j \partial^2 \Psi / \partial x_j^2. \quad (3)$$

Considering the limit $L \rightarrow \infty$, the two-body potential is of the form

$$V = \sum_{i < j} [V_0(x_j - x_i) + V_1(x_j - x_i)],$$